

## Energetics of nanoscale graphene ribbons: Edge geometries and electronic structures

Susumu Okada

*Center for Computational Sciences and Graduate School of Pure and Applied Sciences, University of Tsukuba,  
Tsukuba 305-8571, Japan*

*and CREST, Japan Science and Technology Agency, 4-1-8 Honcho, Kawaguchi, Saitama 332-0012, Japan*

(Received 2 November 2007; published 17 January 2008)

The energetics of nanometer-scale ribbon edges of a monolayer graphite sheet (graphene) is studied by using the local spin density approximation in the density functional theory. The formation energy of an armchair edge is found to be smaller by 1 eV per edge atom than that of a zigzag edge in clean graphene edges. For hydrogenated edges, we also find that the armchair edge is more stable in energy by 0.2 eV per edge atom than the zigzag edge. Atomic configurations at edges and electronic structures near the Fermi level of ribbons are crucial to determine their energetics.

DOI: [10.1103/PhysRevB.77.041408](https://doi.org/10.1103/PhysRevB.77.041408)

PACS number(s): 61.48.-c, 61.46.-w, 68.35.-p, 81.05.Uw

The discovery of fullerenes<sup>1,2</sup> and nanotubes<sup>3</sup> has stimulated both fundamental and technological interest in these nanoscale carbon materials.<sup>4,5</sup> The difference in the global network topology of the carbon materials is known to produce a rich variety of electronic properties: Seamless cylindrical structures result in either metallic or semiconducting properties depending on the helical arrangement of hexagonal networks on the cylinders.<sup>6-8</sup> Further, spherical-harmonic electron states ( $Y_{lm}$ ) emerge on nanoscale “soccer balls”<sup>9</sup> and their condensed phase exhibits superconductivity at high temperature by electron doping.<sup>10-13</sup> These structures comprise a closed network of threefold-coordinated C atoms without any atomistic defects resulting from the twofold-coordinated atoms. Their electronic structures result from the topological defects (pentagons) and boundary conditions that are imposed on the two-dimensional honeycomb network (graphenes).

Graphenes with imperfections (defects and edges) exhibit peculiar electronic properties around the Fermi level.<sup>14-16</sup> In conventional solids with covalent characters, such as Si and diamond, imperfections result in electron states near the Fermi level, which are localized around them due to the unpaired electrons situated at the unsaturated covalent bonds. In the case of graphene, however, the other class of electron states emerges by introducing imperfections due to the presence of two different kinds of electrons, which are concerned with the covalent bond ( $sp^2$ -hybridized states) and the  $\pi$  bond ( $p_z$  states). When graphene flakes or ribbons have edges with a zigzag shape, this causes the emergence of an electron state located at the Fermi energy that is localized near but extended along the edges and lacks dispersion along the edge directions in a part of the Brillouin zone (BZ). The flatband is not peculiar to C atoms, but occurs in hexagonally bonded heterosheets which have borders with zigzag shapes between the chemically different elements.<sup>17</sup> An early analytical study showed that the flatband states (i.e., the edge state or border state) result from a delicate balance of electron transfers among the  $\pi$  orbitals situated near the edge atoms.<sup>14,15</sup> Such edge-localized states near the Fermi level have been indeed observed in a susceptibility measurement experiment<sup>18</sup> and a recent scanning tunneling microscope experiment.<sup>19</sup>

Due to a large Fermi level density of states of the

graphene ribbons with zigzag edges, the ribbon exhibits interesting electronic and magnetic properties, such as peculiar transport properties<sup>20</sup> and magnetism.<sup>21,22</sup> These properties triggered much theoretical and experimental works on graphene flakes with nanometer size.<sup>23-26</sup> While theoretical and experimental studies regarding their electronic properties are advancing steadily, little is known about the fundamentals of the formation and energetics of nanometer-scale graphene flakes. Thus, the purpose of this work is to unravel the energetics of nanometer-size graphene ribbons. In particular, we provide the formation energies of an armchair edge and a zigzag edge for a graphene sheet. Our first-principles total-energy calculations clarify that the formation energy of an armchair edge is smaller than that of a zigzag edge. Moreover, the edge formation energies correlate with the electronic structure of graphene ribbons. Our finding clearly shows that the armchair edge is a favorable structure for edge of nanometer-scale graphene flakes.

All calculations were performed using density functional theory (DFT).<sup>27,28</sup> To express the possibility of the polarization of the electron spin, we treated the exchange-correlation energy of interacting electrons in a local spin density approximation (LSDA) with a functional form<sup>29</sup> fitted to the Ceperley-Alder result.<sup>30</sup> Norm-conserving pseudopotentials generated using the Troullier-Martins scheme<sup>31,32</sup> were adopted to describe the electron-ion interaction. The valence wave functions were expanded by the plane-wave basis set with a cutoff energy of 50 Ry, which gives enough convergence of the relative total energies of carbon-related materials.<sup>33</sup> The conjugate-gradient minimization scheme was used both for the electronic-structure calculation and for the geometry optimization.<sup>34</sup> Structural optimization was performed until the remaining forces were less than 5 mRy/Å. We used the supercell model in which the graphene ribbon is separated by 6 Å and 5 Å in normal and parallel directions to adjacent ribbons, respectively, to simulate an isolated ribbon. Integration over the BZ was carried out using equidistant  $k$ -point sampling in which 12- and 14  $k$  points were taken along a ribbon direction in the armchair and the zigzag edges, respectively.

Figure 1 shows the formation energy ( $\Delta E_C$ ) per edge atom of clean edges on the graphene calculated by

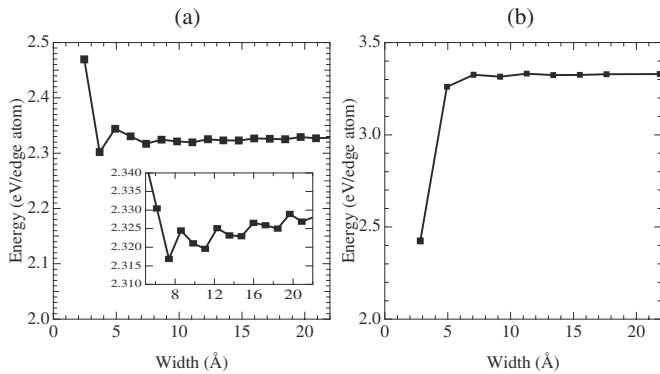


FIG. 1. Formation energies per edge atom of clean edges on a graphene sheet with (a) armchair edges and (b) zigzag edges as a function of the ribbon width. Inset (a), close-up of the formation energy of the armchair edges for the wide ribbons.

$$\Delta E_C = E_{\text{ribbon}}^{\text{tot}} - E_{\text{graphene}}^{\text{tot}},$$

where  $E_{\text{ribbon}}^{\text{tot}}$  and  $E_{\text{graphene}}^{\text{tot}}$  are the total energies of a graphene ribbon and the bulk graphene sheet, respectively. The formation energy of an armchair edge is found to be smaller by about 1 eV per edge atom than that of a zigzag edge, inferring the fact that the clean zigzag edge rarely exists at room temperature under equilibrium conditions. The difference between  $\Delta E_C$  of armchair and zigzag edges is comparable to that obtained in nanotubes edges.<sup>35</sup> The formation energy for the armchair edge exhibits a small but significant width dependence [Fig. 1(a)]. The formation energy oscillates in a triple periodicity of its width and gradually approaches the value of 2.33 eV per edge atom. This dependence results from the electronic structure of ribbons with armchair edges. The fundamental energy gap of these ribbons varies in accordance with a triple periodicity of their width.<sup>14,15,23</sup>

In sharp contrast, the formation energy of the clean zigzag edge is insensitive with respect to its width, except for the ribbon with a width of 3.5 Å [Fig. 1(b)]. It should be noted that the small formation energy of the narrowest zigzag ribbon is ascribed to the spontaneous dissociation of the ribbon into two isolated polyene chains. Thus, the narrowest ribbon with clean zigzag edges is energetically unstable.

To clarify the large difference in the formation energy between the armchair and the zigzag edges, we conducted a detailed study of the geometries of graphene ribbons with armchair and zigzag edges having similar widths. As shown in Fig. 2(a), substantial lattice relaxation takes place on the armchair edge, imparting remarkable stability on the graphene ribbon. It was found that the bond length of the edge C atoms is 1.23 Å, exhibiting the strong pairing nature of the  $sp$  hybridization reported by previous works.<sup>35,36</sup> Indeed, the distribution of valence electrons corroborates this point. The charge density of the edge C-C bonds was higher than the remaining bonds possessing lengths of about 1.4 Å [Fig. 2(a)]. Owing to the strong pairing, the dangling bond nature of the edge C atoms decreases so that the total energy of the ribbon becomes lower. This lower total energy results in the small formation energy of the armchair edge. In sharp

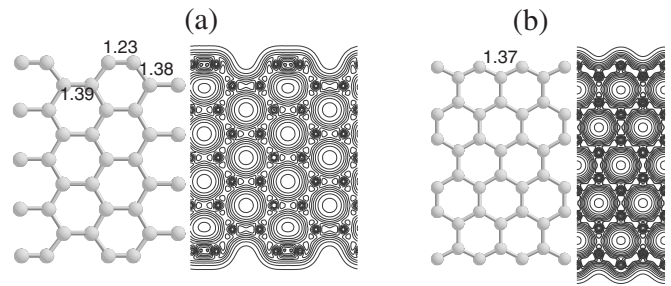


FIG. 2. Optimized geometries and contour plots of total valence electrons of graphene ribbons with (a) clean armchair edges and (b) clean zigzag edges. The difference between each neighbor contour is 0.045 a.u.

contrast, the lattice relaxation at the edge atomic site does not take place for the zigzag edges [Fig. 2(b)]. The calculated bond length of the zigzag edges was found to be 1.39 Å, which is the same as those for atoms with threefold coordination.

It is interesting to understand how the edge formation energy is modulated by the saturating edge dangling bonds. The following focuses on the energetics of the hydrogenated edges to give an answer to the above question. Figure 3 shows the formation energy per edge atom of the hydrogenated zigzag and armchair edges of graphene ribbons. In these cases, the formation energy of the edge ( $\Delta E_H$ ) is calculated by

$$\Delta E_H = E_{\text{ribbon}}^{\text{tot}} - E_{\text{graphene}}^{\text{tot}} - n\mu_H,$$

where  $E_{\text{ribbon}}^{\text{tot}}$ ,  $E_{\text{graphene}}^{\text{tot}}$ ,  $n$ , and  $\mu_H$  represent the total energy of the hydrogenated graphene ribbons, the total energy of the

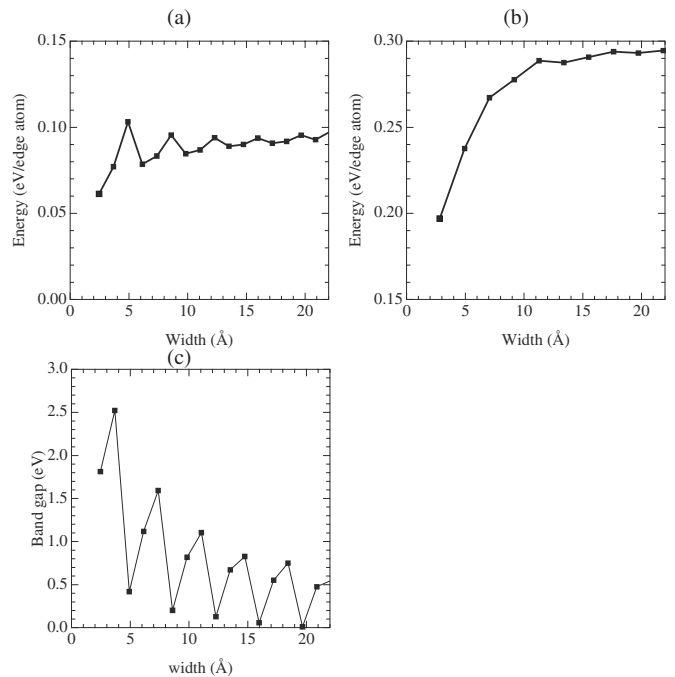


FIG. 3. Formation energies per edge atom of hydrogenated edges on the graphene sheet with (a) an armchair edge and (b) a zigzag edge as a function of the ribbon width. (c) Energy gaps of the ribbons with armchair edges as a function of the ribbon width.

bulk graphene sheet, the number of H atoms, and the chemical potential of the H atom situated in benzene obtained by the energy difference between the total energies of the benzene and the graphene, respectively. In these cases, although each atom situated at the edges is saturated by the H atom resulting in almost the same C-C bond length for the bulk graphite, we find a small but significant difference in their formation energies. The calculated formation energy for the armchair edge is found to be lower by 0.2 eV per edge atom than that of the zigzag edge. The large formation energy of zigzag edges is ascribed to the metallic nature of the ribbons with the zigzag edges. The ribbons possess a large Fermi level density of states which results from flatband states (the edge state) at the Fermi level.<sup>14,15</sup> On the other hand, the ribbons with armchair edges are semiconductors or metals with small density of states at the Fermi level. Thus, in the hydrogenated case, the edge state plays a crucial role in determining the edge structures of the nanometer-scale graphene flakes.

The formation energy is also found to exhibit a width dependence for both the zigzag and armchair edges. In the zigzag edge, the formation energy monotonically increases with increasing ribbon width and gradually approaches the energy of 0.3 eV per edge atom [Fig. 3(b)]. It was found that the ribbons narrower than 10 Å possessed small formation energies resulting from modulation of the electronic structure of the edge states. For these ribbons, the edge states at both edges interact with each other and lose their flatband character at the Fermi level, thereby decreasing the Fermi level density of states.<sup>16</sup> This modulation substantially decreases the edge formation energy.

On the other hand, in the armchair edge, the formation energy exhibits different characteristics from that of the zigzag edge. The energy oscillates around the 0.8 eV with the triple periodicity of the ribbon width [Fig. 3(a)], as in the case of graphene ribbons with clean armchair edges. This oscillation also correlates with the fundamental energy gap of the ribbons with hydrogenated armchair edges:<sup>14,15,23</sup> The maxima and minima of the energies correspond to the ribbons with small band gaps (or metallic for wide ribbons) and large band gaps, respectively [Fig. 3(c)]. From these calculations, we conclude that the edge formation energy also depends on the electronic structure of the ribbons concerning  $\pi$  electrons—i.e., the edge state and energy gap of ribbons—in addition to the dangling bonds at edges resulting in the lattice relaxation.

It is expected that the edge shapes of realistic nanometer-scale graphene flakes are a mixture of zigzag and armchair edges. Here, we examine the energetics of graphene ribbons with a protuberance to simulate the generalized edge structures of graphene flakes. Here, we consider three different protuberances consisting of armchair edges with 120° apices [Fig. 4(a)], mixed edges with 90° apices [Fig. 4(b)], and zigzag edges with 60° apices [Fig. 4(c)]. Figure 4(d) shows the formation energy ( $\Delta E_P$ ) per atom of those protuberances as a function of their height. The formation energy is calculated by

$$\Delta E_P = E_{\text{ribbon}}^{\text{tot}} - E_{\text{graphene}}^{\text{tot}} - n\mu_H - \Delta E_H N_{\text{edge}},$$

where the  $\Delta E_H$  is the formation energy of the zigzag ribbon with width of 7 Å and  $N_{\text{edge}}$  is the number of atoms at the

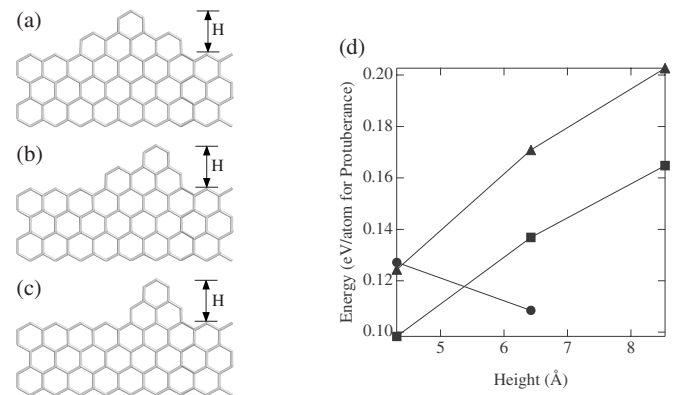


FIG. 4. Optimized geometries of hydrogenated protuberances consisting of (a) armchair (AA) slopes with a 120° apex, (b) an armchair and a zigzag (AZ) slopes with a 90° apex, and (c) the zigzag (ZZ) slopes with a 60° apex. For simplicity, hydrogen atoms are omitted in each figure. (d) Formation energies of the hydrogenated protuberances as a function of their height. Solid circles, squares, and triangles denote the energies for the AA, AZ, and ZZ protuberances, respectively.

parallel edges. As shown in Fig. 4(d), the formation energy does not depend on the apex angle for the smallest protuberance studied here. In sharp contrast, by increasing the height of the protuberances, the formation energy exhibits different characteristics for each edge. The energy is almost independent of the height for the protuberance consisting of armchair edges. This feature is ascribed to the fact that the formation energy of the armchair edge does not depend on the ribbon width. On the other hand, in the protuberances containing zigzag edges, the energy monotonically increases by increasing the height. As pointed out in the graphene ribbons with hydrogenated zigzag edges, the formation energy of the zigzag edge strongly depends on its width for narrow ribbons due to the modulation of the edge states at the Fermi level. Based on the results, it is inferred that the edges of realistic graphene flakes mainly consist of armchair edges with a small portion of zigzag edges exceptionally introduced under the formation conditions. Perhaps, the zigzag region is not more than two or three units in the realistic graphene edge. These results agree well with the recent experimental result that armchair edges are dominantly observed in nanometer-scale graphene flakes by a scanning tunneling microscope.<sup>19</sup> Furthermore, the results also agree well with a previous theoretical calculation that the armchair edge is more favorable for the graphene ribbons.<sup>37</sup>

In summary, we find that the armchair edge of the graphene ribbon is more stable in energy than the zigzag edge. Our calculations show that the formation energy of the armchair edge is smaller by 1.0 eV per edge atom than that of the zigzag edge for the clean ribbon edges. The remarkable stability of the armchair edge is ascribed to the strong paring of the edge atoms resulting in the formation of a triple bond between them. For the hydrogenated edges, we also find that the formation energy of the armchair edge is smaller by 0.2 eV per edge atom than that of the zigzag edge. The energy difference results from the edge state situated at the zigzag edge, resulting in half-filled flatbands at the Fermi

level. Our results provide a theoretical explanation for the experimental fact that the armchair edge is dominant for nanometer-scale graphene flakes. For edges with a more generalized shape, we demonstrate that hybrid edges consisting of armchair-type edge and short zigzag-type edges are plausible edge structures in a realistic situation.

This work was partly supported by CREST-JST and a grant-in-aid for scientific research from the MEXT Japan. Computations were performed on NEC SX series at CCS, University of Tsukuba, at YITP, Kyoto University, at CMC, Osaka University, at ISC, Tohoku University, and at RCCS, Okazaki National Institute.

- <sup>1</sup>H. W. Kroto, J. R. Heath, S. C. O'Brien, R. F. Curl, and R. E. Smalley, *Nature (London)* **318**, 162 (1985).
- <sup>2</sup>W. Krätschmer, K. Fostiropoulos, and D. R. Hoffman, *Nature (London)* **347**, 354 (1990).
- <sup>3</sup>S. Iijima, *Nature (London)* **354**, 56 (1991).
- <sup>4</sup>M. S. Dresselhaus, G. Dresselhaus, and P. C. Eklund, *Science of Fullerenes and Carbon Nanotubes* (Academic Press, San Diego, 1996).
- <sup>5</sup>R. Saito, G. Dresselhaus, and M. S. Dresselhaus, *Physical Properties of Carbon Nanotubes* (Imperial College Press, London, 1998).
- <sup>6</sup>N. Hamada, S.-I. Sawada, and A. Oshiyama, *Phys. Rev. Lett.* **68**, 1579 (1992).
- <sup>7</sup>R. Saito, M. Fujita, M. S. Dresselhaus, and G. Dresselhaus, *Appl. Phys. Lett.* **60**, 2204 (1992).
- <sup>8</sup>J. W. Mintmire, B. I. Dunlap, and C. T. White, *Phys. Rev. Lett.* **68**, 631 (1992).
- <sup>9</sup>S. Saito and A. Oshiyama, *Phys. Rev. Lett.* **66**, 2637 (1991).
- <sup>10</sup>A. F. Hebard, M. J. Rosseinsky, R. C. Haddon, D. W. Murphy, S. H. Glarum, T. T. M. Palstra, A. P. Ramirez, and A. R. Kortan, *Nature (London)* **350**, 632 (1991).
- <sup>11</sup>M. J. Rosseinsky, A. P. Ramirez, S. H. Glarum, D. W. Murphy, R. C. Haddon, A. F. Hebard, T. T. M. Palstra, A. R. Kortan, S. M. Zahurak, and A. V. Makhija, *Phys. Rev. Lett.* **66**, 2830 (1991).
- <sup>12</sup>P. W. Stephens, L. Mihaly, P. L. Lee, R. L. Whetten, S. Huang, R. Kaner, F. Deiderich, and K. Holczer, *Nature (London)* **351**, 632 (1991).
- <sup>13</sup>K. Tanigaki, T. W. Ebbesen, S. Saito, J. Mizuki, J. S. Tsai, Y. Kubo, and S. Kuroshima, *Nature (London)* **352**, 222 (1991).
- <sup>14</sup>M. Fujita, L. Wakabayashi, K. Nakada, and K. Kusakabe, *J. Phys. Soc. Jpn.* **65**, 1920 (1996).
- <sup>15</sup>K. Nakada, M. Fujita, G. Dresselhaus, and M. S. Dresselhaus, *Phys. Rev. B* **54**, 17954 (1996).
- <sup>16</sup>Y. Miyamoto, K. Nakada, and M. Fujita, *Phys. Rev. B* **59**, 9858 (1999).
- <sup>17</sup>S. Okada, M. Igami, K. Nakada, and A. Oshiyama, *Phys. Rev. B* **62**, 9896 (2000).
- <sup>18</sup>Y. Shibayama, H. Sato, T. Enoki, and M. Endo, *Phys. Rev. Lett.* **84**, 1744 (2000).
- <sup>19</sup>Y. Kobayashi, K.-I. Fukui, T. Enoki, and K. Kusakabe, *Phys. Rev. B* **73**, 125415 (2006).
- <sup>20</sup>K. Wakabayashi, Y. Takane, and M. Sigrist, *Phys. Rev. Lett.* **99**, 036601 (2007).
- <sup>21</sup>S. Okada and A. Oshiyama, *Phys. Rev. Lett.* **87**, 146803 (2001).
- <sup>22</sup>S. Okada and A. Oshiyama, *J. Phys. Soc. Jpn.* **72**, 1510 (2001).
- <sup>23</sup>Y.-W. Son, M. L. Cohen, and S. G. Louie, *Phys. Rev. Lett.* **97**, 216803 (2006).
- <sup>24</sup>Y.-W. Son, M. L. Cohen, and S. G. Louie, *Nature (London)* **444**, 347 (2006).
- <sup>25</sup>T. Enoki and K. Takai, in *Carbon-Based Magnetism*, edited by T. L. Makarova and F. Palacio (Elsevier, Amsterdam, 2006), p. 397.
- <sup>26</sup>K. Wakabayashi, in *Carbon-Based Magnetism*, edited by T. L. Makarova and F. Palacio (Elsevier, Amsterdam, 2006), p. 279.
- <sup>27</sup>P. Hohenberg and W. Kohn, *Phys. Rev.* **136**, B864 (1964).
- <sup>28</sup>W. Kohn and L. J. Sham, *Phys. Rev.* **140**, A1133 (1965).
- <sup>29</sup>J. P. Perdew and A. Zunger, *Phys. Rev. B* **23**, 5048 (1981).
- <sup>30</sup>D. M. Ceperley and B. J. Alder, *Phys. Rev. Lett.* **45**, 566 (1980).
- <sup>31</sup>N. Troullier and J. L. Martins, *Phys. Rev. B* **43**, 1993 (1991).
- <sup>32</sup>L. Kleinman and D. M. Bylander, *Phys. Rev. Lett.* **48**, 1425 (1982).
- <sup>33</sup>S. Okada, S. Saito, and A. Oshiyama, *Phys. Rev. Lett.* **86**, 3835 (2001).
- <sup>34</sup>O. Sugino and A. Oshiyama, *Phys. Rev. Lett.* **68**, 1858 (1992).
- <sup>35</sup>Y.-H. Lee, S.-G. Kim, and D. Tomanek, *Phys. Rev. Lett.* **78**, 2393 (1997).
- <sup>36</sup>L. R. Radovic and B. Bockrath, *J. Am. Chem. Soc.* **127**, 5917 (2005).
- <sup>37</sup>V. Varone, O. Hod, and G. E. Scuseria, *Nano Lett.* **6**, 2748 (2006).